ARTICLE

Theoretical Investigation on Triplet Excitation Energy Transfer in Fluorene Dimer[†]

Yu-bing Si, Xin-xin Zhong, Wei-wei Zhang, Yi Zhao*

State Key Laboratory of Physical Chemistry of Solid Surfaces, Fujian Provincial Key Lab of Theoretical and Computational Chemistry, College of Chemistry and Chemical Engineering, Xiamen University, Xiamen 361005, China

(Dated: Received on August 11, 2011; Accepted on September 16, 2011)

Triplet-triplet energy transfer in fluorene dimer is investigated by combining rate theories with electronic structure calculations. The two key parameters for the control of energy transfer, electronic coupling and reorganization energy, are calculated based on the diabatic states constructed by the constrained density functional theory. The fluctuation of the electronic coupling is further revealed by molecular dynamics simulation. Succeedingly, the diagonal and off-diagonal fluctuations of the Hamiltonian are mapped from the correlation functions of those parameters, and the rate is then estimated both from the perturbation theory and wavepacket diffusion method. The results manifest that both the static and dynamic fluctuations enhance the rate significantly, but the rate from the dynamic fluctuation is smaller than that from the static fluctuation.

Key words: Triplet excitation energy transfer, Constrained density functional theory, Marcus formula, Wavepacket diffusion method

I. INTRODUCTION

Energy transfer is widely involved in many different areas from biological to chemical reactions, leading to a remarkable interest in both theory and experiment [1−7]. In typical organic electronics, the energy transfer is a key process and the charge injection generally leads to a 3:1 ratio of triplet to singlet excitons by spin statistics, which implies that 75% of the created excitons will be phosphorescent rather than luminescent. Furthermore, the engineering greater fractions of triplet excitons might be a route to improve the short singlet exciton diffusion lengths. Therefore, the triplet-triplet energy transfer (TTET) becomes significant in the design of organic photovoltaic devices.

Recently, Weis *et al.* have synthesized a series of π-stacked molecules consisting of a benzophenone donor, three fluorene bridges, and a naphthalene acceptor, and measured the TTET rates from benzophenone to naphthalene across the fluorene bridges [8]. It is found that TTET has a crossover from single-step tunneling to multi-step hopping with the increasing of the bridge length. Theoretically, Voityuk has investigated TTET rate between adjacent fluorenes, shown in Fig.1, in a short π stack [9]. Combining the quantum chemistry calculations for the electronic coupling and reorganization energy with Marcus rate formula, he has calculated the TTET rate. This theoretical investigation is helpful to understand the relationship between the molecular structure and energy transfer yield.

In the present work, we also focus on the TTET between fluorenes. However, we dominantly investigate the dynamic disorder effect on the TTET, which is different from Voityuk's one [9]. Concretely, we use a wavepacket diffusion method proposed by us to incorporate the dynamic disorder. The approach is beyond the perturbation theory and especially suitable when the dynamic disorder becomes strong. Meanwhile, the partial quantum effect of the nuclear motions can be incorporated compared to the classical molecular dynamics (MD) simulation.

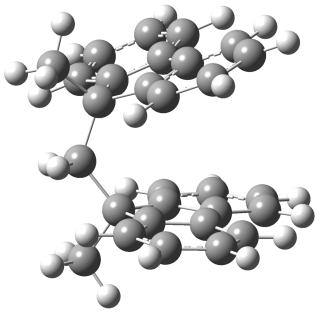

FIG. 1 Structure of the fluorene dimer optimized at the B3LYP/6-31G* level.

[†]Part of the special issue for "the Chinese Chemical Society's 12th National Chemical Dynamics Symposium".

*Author to whom correspondence should be addressed. E-mail: yizhao@xmu.edu.cn

It is known that the flexibility of the spacer or linker between the energy donor and accepting groups has significant effects on the mechanism and rates of energy transfer. For instance, in the study of the mobility in organic crystals, the calculations from *ab initio* method and classical MD have demonstrated that the averaged value of the electronic coupling and its thermal fluctuation are of the same order of magnitude [10]. It manifests that the charge carrier is localized by the dynamic off-diagonal disorder which is quite different from the localization due to the reorganization energy. The predicted mobility shows bandlike property and the mean free path has a reasonable value. Recently, we have proposed the analytical rate expressions involving the dynamic disorder with use of Fermi's golden rule, and found that the Marcus parabolic shape is dramatically changed [11]. In this work, therefore, we reveal this effect on the TTET rates in the fluorene dimer.

Another purpose of the present paper is to find out an easy, and accurate way to calculate the electronic coupling and reorganization energy, which are two key parameters for the control of energy transfer. It is known that these parameters are heavily dependent on the choice of the diabatic states. Voityuk [9] has used the fragment excitation difference (FED) approach proposed by Hsu [12]. In this work, we use the constrained density functional theory (CDFT) approach [13, 14] where the net spin on the part of donor and acceptor can be easily constrained, and the diabatic states can be explicitly performed. Moreover, we investigate the mode-specific reorganization energy, which can reveal the more detailed structure-property relationship of the devices.

In this work, we briefly summarize the wavepacket diffusion method for dynamics with disorder and electronic structure methods for the calculations of electronic coupling and reorganization energy.

II. COMPUTATIONAL METHODS

A. Wavepacket diffusion method

A time-dependent wavepacket diffusion method is originally proposed to deal with charge transport in organic crystals. It can be straightforwardly applied to the TTET. In the approach, electron-phonon interactions in both site energies and electronic couplings are incorporated by the time-dependent fluctuations that are generated from the corresponding spectral density functions. Here, we outline the working expression. The Hamiltonian for a dimer can be written as follows [15, 16]:

$$H(t) = \sum_{i=1}^{2} \left[\varepsilon_{ii} + V_{ii}(t)\right] |i\rangle \langle i| + \sum_{i\neq j}^{2} \left[\varepsilon_{ij} + V_{ij}(t)\right] |i\rangle \langle j| \quad (1)$$

where ε_{ii} and ε_{ij} ($i\neq j$) are the static site energies and electronic couplings between sites respectively, and the fluctuations of the site energies and electronic couplings are denoted by $V_{ii}(t)$ and $V_{ij}(t)$ respectively. It is easily demonstrated that these time-dependent fluctuations correspond to the quantum electron-phonon interactions in the interaction representation. In the classical approximation, $V_{ii}(t)$ and $V_{ij}(t)$ can be created from their spectral density functions [17−19].

$$H(t) = \sqrt{2}\sum_{n=1}^{N} \sqrt{2G(\omega_n)\Delta\omega}\cos(\omega_n t + \phi_n) \quad (2)$$

where the spectral density function $G(\omega)$ is correlated by the correlation function,

$$\begin{aligned} G_{cl}(\omega) &= \frac{1}{2\pi}\int_{-\infty}^{+\infty} \mathrm{d}t \exp(i\omega t) C_{cl}(t) \\ &= \frac{1}{2\pi}\int_{-\infty}^{+\infty} \mathrm{d}t \exp(i\omega t) \langle \delta V(t)\delta V(0)\rangle \end{aligned} \quad (3)$$

here, the fluctuation of the electronic couplings $\delta V(t)$ can be obtained from the MD simulation. Their correlation functions are defined by

$$C_{cl}(t) = \langle \delta V(t)\delta V(0)\rangle \quad (4)$$

where the brackets $\langle\rangle$ represent the fluctuation average. However, it is noted that the correlation function should be complex generally and satisfy the detailed balance. To incorporate this quantum effect, one may modify the classical spectral density function by [20],

$$G(\omega) = \frac{2G_{cl}(\omega)}{1+\exp(-\beta\hbar\omega)} \quad (5)$$

where β=1/($k_{\mathrm{B}}T$) and T is temperature. Once the time-dependent Hamiltonian elements are constructed, the charge carrier dynamics can be obtained by solving the Schrödinger equation,

$$i\hbar\frac{\partial\varphi(t)}{\partial t} = H(t)\varphi(t) \quad (6)$$

The formal solution of the wave function $\varphi(t)$ is written by

$$\begin{aligned} \varphi(t) &= U(t)\varphi(0) \\ &= T\exp\left[-\frac{i}{\hbar}\int_0^t H(t')\mathrm{d}t'\right]\varphi(0) \end{aligned} \quad (7)$$

where $U(t)$ is the time-evolution operator and T is the time-ordering operator. Numerically, the time-evolution operator is commonly splitted into small increments of duration Δt in which the variation of the Hamiltonian operator is small. Thus, $U(t)$ is expressed as

$$U(t) = \prod_{0}^{N-1} U[(n+1)\Delta t, n\Delta t] \quad (8)$$

DOI:10.1088/1674-0068/24/05/538-546

where Δt=t/N and

$$U(t+\Delta t,t)=\exp\left[-\frac{i}{\hbar}H(t)\Delta t\right] \tag{9}$$

here, we expand $U(t)$ with Chebyshev polynomials for the propagation [21, 22] and the short time propagator is written as

$$U(t+\Delta t,t)=\sum_{0}^{+\infty}\exp\left(-i\frac{a\Delta t}{\hbar}\right)h_n i^n J_n\cdot \left(-\frac{b\Delta t}{\hbar}\right)T_n\left[\frac{H(t)-a}{b}\right] \tag{10}$$

where T_n is the first-kind Chebyshev polynomials, J_n is Bessel functions, the energy spectrum of H has the interval [a−b, a+b], and h_0=1, h_n=2 (n>0). The higher-order T_n can be obtained by the recursive relation.

Expanding the wave function in the site representation

$$\varphi(t)=\sum_{i}^{N}c_i(t)\,|i\rangle \tag{11}$$

one may obtain coefficients $c_i(t)$ from initial values $c_i(0)$. Therefore, the population dynamics $\rho_{ii}(t)$ on the ith site, *i.e.*, wavepacket motion, is straightforwardly given by

$$\rho_{ii}(t)=\langle c_i^*(t)c_i(t)\rangle \tag{12}$$

where $\langle\rangle$ represents the statistic average.

As the electronic population dynamics shows the exponential relaxation toward the equilibrium state, the TTET rate is described by the following kinetic equations [23],

$$\dot{\rho}_{11}(t)=-k_1\rho_{11}(t)+k_2\rho_{22}(t) \tag{13}$$

$$\dot{\rho}_{22}(t)=k_1\rho_{11}(t)-k_2\rho_{22}(t) \tag{14}$$

where k_1 and k_2 are the forward and back TTET rate, respectively. For the symmetric systems, the forward and back rate are the same and the above kinetic equations are rewritten by

$$\dot{P}(t)=-2k_1P(t) \tag{15}$$

$$k_1(t)=-\frac{1}{2}\frac{\dot{P}(t)}{P(t)} \tag{16}$$

here, the population difference $P(t)$=$\rho_{11}(t)-\rho_{22}(t)$. As long as the above definition of rate is meaningful, the time-dependent decay rate $k_1(t)$ will reach the plateau value after a certain time t_p. This asymptotic value corresponds to the TTET rate $k_{\rm TTET}$,

$$k_{\rm TTET}=\lim_{t\to t_p}k_1(t)=-\frac{1}{2}\lim_{t\to t_p}\frac{{\rm d}\ln P(t)}{{\rm d}t} \tag{17}$$

B. Reorganization energy and electronic coupling

It is known that the spectral density functions of the fluctuations of the diagonal and off-diagonal elements in the Hamiltonian are explicitly correlated to the reorganization energy and electronic coupling. We show here electronic structure methods for their calculations.

The reorganization energy in TTET is the energy cost due to geometry modifications to go from a triplet to a singlet states and vice versa. Therefore, it is not sensitive to the geometric arrangements between two monomers. An easy way to calculate the reorganization energy is the four-point technique proposed by Nelsen [24], which has been identified as a reliable tool by our previous study on the electron transfer (ET) process in organic radicals [25, 26]. For this neutral TTET process, the molecule is splitted into the neutral triplet donor and singlet acceptor parts which are calculated separately or can be taken as a whole to calculate. If we use opt and fc to represent the optimized states and Franck-Condon excited states, the spin multiplicity is labeled as the superscript, and the reorganization energy is then given by

$$\lambda=[E(D^{\rm T}_{\rm fc})-E(D^{\rm T}_{\rm opt})]+[E(A^{\rm S}_{\rm fc})-E(A^{\rm S}_{\rm opt})] \tag{18}$$

where S and T represent the optimized geometries of singlet and triplet state, respectively. Alternatively, the reorganization energy can be calculated by

$$\lambda=\frac{1}{2}\sum_i{\omega_i}^2{\Delta Q_i}^2 \tag{19}$$

where ΔQ_i represents the normal-mode coordinate shift between the donor and acceptor states, and ω_i represents the frequency for the ith mode. This mode-specific reorganization energies are more interesting because they can reveal significant modes for the contributions of TTET. In addition, they explicitly relate to the dynamic disorder of the site energies. In the numerical calculation, the frequency of each mode can be obtained at the optimized geometry from many *ab initio* software packages, and ΔQ_i can be obtained by the matrix transformation techniques [27−31].

For the electronic coupling, however, the conformational changes dramatically affect its value. To obtain the dimer geometries for the calculation of the electronic coupling as well as its correlation function, we employ the standard NVE ensemble protocol and the program AMBER to implement the MD simulation [32]. To increase the accuracy, the fluorene dimer is optimized at the B3LYP/6-31G* level instead of the HF/6-31G* with Gaussian 09 program [33]. After the RESP atomic charges at the B3LYP/cc-pVTZ level [34] are obtained, the MD simulation is performed as follows: 10 ps simulation at 300 K, 1 fs integration step, GAFF force field [35], cutoff of 15 Å for nonbonded interactions. During the simulation, 1000 snapshots separated by 50 fs are saved for the electronic coupling calculations.

DOI:10.1088/1674-0068/24/05/538-546

At a given geometry, the electronic coupling is commonly calculated from the diabatic representation and the adiabatic representation. For example, the FED [12] and the fragment spin difference (FSD) approaches [36] are from the adiabatic-based way. Alternatively, the CDFT approach is based on the diabatic representation. In the adiabatic-based approaches, one has to carefully select the proper excited states as well as transition densities from CIS/TDDFT. If the incorrect adiabatic states are chosen, the diabatic-adiabatic transformation will fail to yield the appropriate electronic coupling. On the contrary, the diabatic-based approach may easily constrain the spin or charge to generate the diabatic states. In this work, we choose the CDFT method which can be straightforwardly used to calculate the electronic coupling for TTET, although other methods are also used for a purpose of comparison. In the CDFT, it is easy to constrain the spin up and spin down densities in a measure of the net spin on the part of donor and acceptor. Once the spin is localized on the fragments, *i.e.*, the diabatic states, the electronic coupling can be obtained by

$$V_{rp} = \frac{H_{rp} - S_{rp}(E_r + E_p)/2}{1 - {S_{rp}}^2} \tag{20}$$

where E_r and E_p are the diabatic state energies, H_{rp} and S_{rp} are the electronic coupling and the overlap matrix of the diabatic state respectively,

$$H_{rp} = \langle D^{\mathrm{T}}A|\hat{H}|DA^{\mathrm{T}}\rangle \tag{21}$$

$$S_{rp} = \langle D^{\mathrm{T}}A \,|\, DA^{\mathrm{T}}\rangle \tag{22}$$

In the process of TTET, $D^{\mathrm{T}}A$ and DA^{T} are corresponding to the triplet states which localized on the donor and acceptor molecule, respectively.

III. NUMERICAL RESULTS

A. Reorganization energy

The calculation of the reorganization energy needs the spin localized diabatic states. Although the HF method can determine these states by the optimization, it neglects electron correlation, and commonly leads to a larger reorganization energy than the experimentally measured one. The DFT approach with a suitable function may predict a reasonable reorganization energy. However, it meets a challenge to find the well-defined charge-separated and spin localized diabatic states. In the present work, we initially use the geometric guess from the CDFT calculation to construct the diabatic states by the DFT optimization, and the obtained diabatic state fortunately has a correct property that the triplet excitation is localized on a single fluorene fragment. It is known that the DFT with the conventional functionals provides a poor description of the π-stacked systems, due to the known problems on the nonlocality and asymptotic behavior of available density functionals [37−39]. Therefore, we test different functionals with the 6-31G* basis set to calculate the reorganization energy, and the results are shown in Table I.

TABLE I Reorganization energy calculations from different methods.

Methods	λ/eV	χ[a]
HF	2.01	100
B3LYP	0.95	20
X3LYP	0.97	21.8
ωB97X-D[b]	1.25	22(S)
		100(L)
M05-2X	1.23	56
M06-HF	1.58	100
M06-2X	1.20	54

[a] χ is percentage of HF exchange in the functional.
[b] For the ωB97X-D functional, 22(S) and 100(L) represent the 22% of HF-like exchange at short-range and 100% at long-range, respectively.

It is seen that the pure HF predicts the highest reorganization energy, which is consistent with our previous conclusion [25, 26]. Compared to B3LYP and X3LYP, the long-range-corrected functional ωB97X-D [40] shows 30% higher. This difference may be caused by the unsuitable optimized μ value for the present system. In addition, we also test the hybrid meta generalized gradient approximation (HM-GGA), such as M05-2X, M06-2X, and M06-HF functionals with Grid=UltraFineGrid [41], and the results manifest that increasing the percentage of HF exchange in the functional leads to an increase of reorganization energy.

It is noted that Voityuk has used the variance of the energy difference of donor and acceptor from CIS/6-31G* along the MD trajectory to derive the reorganization energy. The obtained result is about 0.37 eV [9], which is much smaller than the present values. It is not clear yet what produces such a big difference. To guarantee the present value reasonable, however, we further calculate the vertical excitation energy at the optimized diabatic geometry. In this case, the excitation energy exactly corresponds to the reorganization energy if the parabolic approximation is satisfied. This energy (0.95 eV) from the B3LYP is indeed consistent with the four-point calculation.

Moreover, we have calculated the mode-specific reorganization energy with use of the B3LYP. The result is shown in Fig.2. It is noted that only several modes (the vibration of C−C/C=C bond) have large reorganization energies. Especially, the mode with a frequency of 1697.3 cm^{-1} has extremely large reorganization energy. In the rate calculation, we will show its effect on the rate. It is more interesting that the total reorganization energy from this approach is 0.94 eV, which again

DOI:10.1088/1674-0068/24/05/538-546

TABLE II The electronic coupling calculation from different methods[a].

	FED		CDFT				
	HF-CIS	B3LYP	B3LYP	X3LYP	M05-2X	M06-HF	M06-2X
Coupling/meV	5.5	85.2	5.6	5.7	5.8	5.3	5.4

[a] The FED data are calculated by Q-Chem package [42] while the CDFT method are from NW-Chem program [43], and the basis set used are all 6-31G*.

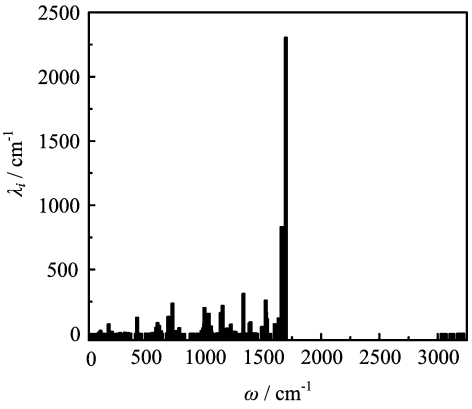

FIG. 2 Reorganization energy components as a function of frequency.

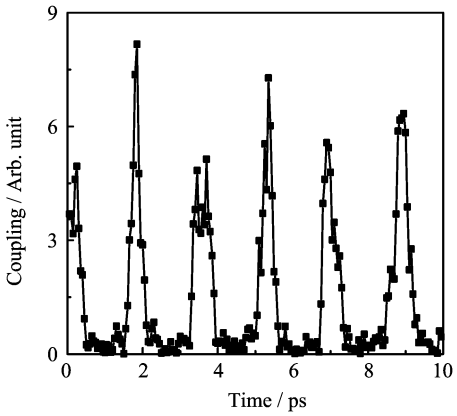

FIG. 3 Fluctuation of the TTET coupling of the fluorene dimer.

agrees very well with those from the four-point model and the vertical excitation calculations.

B. Electronic coupling

In the calculation of electronic coupling, we use several available approaches for a purpose of comparison. Table II lists the obtained results at the optimized diabatic geometry from the CDFT.

One can find from Table II that the FED based on the adiabatic states from the Hartree-Fock configuration-interaction singles (HF-CIS) predicts the similar data with the CDFT method. It can be easily understood from the variational principle of CDFT. When the Beck's atomic partitioning scheme [44] is added in the exchange part of DFT, which brings the CDFT "shift" to the HF formalism, the CDFT thus becomes a constrained HF (CHF) method [45]. In another word, the CDFT is more like HF than the regular DFT functionals. It is known that the time-dependent DFT (TDDFT) fails to describe the polarizabilities of large π-conjugated systems and the long-range ET excitations [46−48]. Therefore, it is not surprised to see the electronic coupling from the B3LYP with the FED model is much large.

In the experimental measurement, the electronic coupling between the monomers is very small and cannot be over 0.01 eV at 77 K [8]. Since the electronic couplings in Table II are at the temperature of 0 K, the value from the FED with the B3LYP is definitely too large. Therefore, we conclude that the CDFT method is a robust tool to calculate the electronic coupling for TTET.

However, the TTET rate is measured at the room temperature. To investigate the fluctuation of the geometry on the rate, we run the MD simulation for the fluorene dimer at the room temperature, and select 200 snapshot structures from the MD trajectory. At each geometry, we calculate the electronic coupling by the CDFT with B3LYP functional.

Figure 3 displays the electronic coupling fluctuation with respect to the MD simulation time. It is clearly seen that the geometry fluctuation significantly change the electronic coupling at the stable geometry, for instance, the maximum electronic coupling can be 30 times as large as that at the stable geometry. Moreover, with time passing by, the electronic coupling presents the periodic property, which can be easily explained from the molecular structure. From the MD simulations, we find that the fluorene monomers are nearly parallel after about the same time interval, where the orbital overlap reaches a maximum and the electronic coupling becomes large.

As the fluctuation of the electronic coupling is much slower than the energy transfer, an averaged electronic coupling is introduced to measure coupling strength, and it is defined by

$$V_{\rm rms} = \sqrt{\langle V^2 \rangle}$$

DOI:10.1088/1674-0068/24/05/538-546

$$= \sqrt{\frac{1}{n}\sum_{1}^{n} {V_i}^2} \quad (23)$$

where V_i is the electronic coupling at the ith geometry. The data in Fig.3 leads to the averaged electronic coupling of 67 meV. Compared to 5.6 meV at the stable geometry, the averaged electronic coupling is about 10 times larger, manifesting that the fluctuation helps energy transfer. Indeed, the rate will enhance 100 times under the perturbation limit by this sole fluctuation. Compared to the value (0.02 eV) obtained by Voityuk [9], our result is three times larger. These difference again comes from the choices of the diabatic states and the quantum chemistry methods. In the present calculations, we rigorously use CDFT to get the correct diabatic states with DFT while the FED approach with HF-CIS used by Voityuk depends on the choices of adiabatic excitation states [9].

C. TTET rate

With use of the obtained reorganization energy and electronic coupling, we can calculate the TTET rate. For a comparison, we start from the well-known Marcus formula [49, 50] in the non-adiabatic high-temperature limit,

$$k(T) = \frac{2\pi}{\hbar} V^2 \sqrt{\frac{1}{4\pi\lambda k_{\mathrm{B}} T}} \exp\left[-\frac{(\Delta G + \lambda)^2}{4\lambda k_{\mathrm{B}} T}\right] \quad (24)$$

here, ΔG is the total change in free energy between the final and initial states. For the fluorene dimer, ΔG=0 because of the symmetric donor and acceptor. In the numerical calculation, we use the reorganization energy of 0.94 eV, and the averaged electronic coupling of 67 meV, both of which come from the calculations of the CDFT with B3LYP functional. The obtained TTET rate is 8.7×10^9 s^{-1}.

From the mode-specific reorganization energy, however, it is known that the modes with high frequencies have the dominant contribution to the total reorganization energy (see in Fig.2). One thus expects that the nuclear tunneling becomes important. To incorporate this effect, we use the rigorous Fermi's golden rule to estimate the rate. The corresponding rate [51] is

$$k(T) = \frac{V^2}{\hbar^2} \int_{-\infty}^{\infty} \mathrm{d}t C(t) \quad (25)$$

with the time-dependent correlation function

$$C(t) = \exp\left\{\frac{-i\Delta G t}{\hbar} - S[(2n+1) - n\exp(i\omega t) - (n+1)\exp(-i\omega t)]\right\} \quad (26)$$

where n=[exp($\beta\omega$) − 1]$^{-1}$, and Huang-Rhys factor S=$\lambda/\hbar\omega$. Furthermore, we can obtain an analytical rate expression for the one-mode system by the integration over time in Eq.(25) as follows

$$k(T) = \frac{2\pi V^2}{\hbar^2\omega}\left(\frac{n+1}{n}\right)^{p/2} \exp[-S(2n+1)] \cdot I_p\{2S[n(n+1)]^{1/2}\} \quad (27)$$

where p=$\Delta G/\hbar\omega$, I_p is modified Bessel function.

In the application, we map the present multi-modes to an effective mode [52]. The effective frequency is 1453 cm^{-1}. The obtained rate is 1.285×10^{12} s^{-1}. Compared to the rate from the Marcus formula, quantum effect enhances the rate about 150 times.

Although we use the perturbation theory to obtain the rate, it is not clear whether the perturbation approximation is valid. To make a judgment, we find that $4V/\lambda$=0.28 is smaller than 1, manifesting the localized property [53]. With our previous work [52], however, it seems that the perturbation approximation reaches its up limit even if it works in the present case. Therefore, it is necessary to use the approach beyond the perturbation limit to rigorously estimate the rate. In the following, we use the wavepacket diffusion approach to calculate the rate. The approach not only overcomes the perturbation limit, but also easily incorporates the dynamic disorder although the fluctuation is involved by a classical way. It has been confirmed that the spin-boson dynamics can be correctly predicted, which guarantees the accuracy for the application to the present system.

To construct the fluctuation from the reorganization energy and time-dependent electronic couplings, we start from the spectral density functions. For the site energy fluctuation, the corresponding spectral density is defined by

$$J(\omega) = \frac{\pi}{2}\sum_j \frac{{c_j}^2}{\omega_j}\delta(\omega - \omega_j) \quad (28)$$

where ω_j and c_j represent the frequency of the jth phonon mode and its electron-phonon interaction strength, respectively. From the mode-specific reorganization energies, we can obtain the spectral density $J(\omega)$ in Eq.(28) by

$$\Delta Q_j = \frac{c_j}{{\omega_j}^2} \quad (29)$$

Then the discrete spectral density is smoothed to a continuous line. The quantum correlation function of $V_{ii}(t)$ in Eq.(1) is given by

$$C_{qu}(t) = \frac{1}{\pi}\int_{-\infty}^{+\infty} \mathrm{d}\omega \frac{\exp(-i\omega t)J(\omega)}{1-\exp(-\beta\omega)} = \int_{-\infty}^{+\infty} \mathrm{d}\omega \exp(-i\omega t)G(\omega) \quad (30)$$

$$G(\omega) = \frac{J(\omega)}{\pi[1-\exp(-\beta\omega)]} \quad (31)$$

DOI:10.1088/1674-0068/24/05/538-546

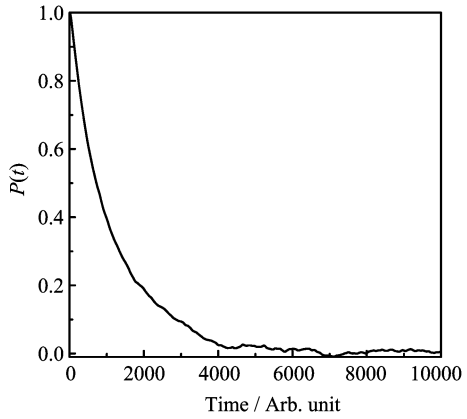

FIG. 4 Time dependence of population difference $P(t)$ with pure diagonal disorder at T=300 K.

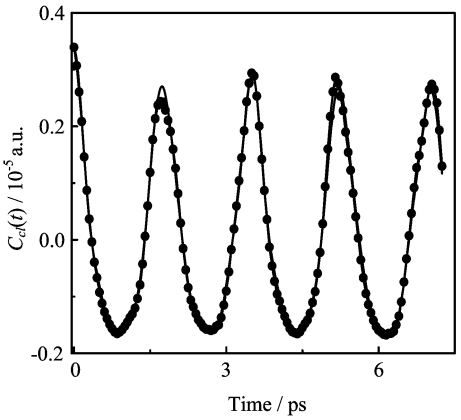

FIG. 5 The classical time correlation function of electronic coupling. The chain-dotted and solid lines are the results from the MD data and Fourier transform of the spectral density $G_{cl}(\omega)$, respectively.

The corresponding site energy fluctuation can be obtained by Eq.(2).

First, we investigate the energy transfer dynamics by neglecting the electronic coupling fluctuation only with the averaged electronic coupling. Figure 4 displays the time-dependence of population difference $P(t)$. It is clearly seen that the population decays exponentially and the coherent motion from the delocalization is not important. Therefore, we can get the rate from the population dynamics. The result is 1.724×10^{13} s^{-1}.

Compared to the rates from the Marcus and Fermi's golden rule, the rate from the wavepacket calculation is explicitly large, manifesting the perturbation theory underestimates the rate for the present system.

It is more interesting to know the effect of electronic coupling disorder on the rate. To construct the fluctuation, we first calculate the classical time correlation function of electronic coupling with the results of MD simulation. The result is shown in Fig.5. It is seen that the correlation function shows the oscillation properties with time, which is consistent with the MD data of electronic coupling (Fig.3). In addition, we can see from Fig.5 that the correlation function from the Fourier transform of the spectral density $G_{cl}(\omega)$ in Eq.(3) agrees well with the one from $V(t)$, which demonstrates that the spectral density $G_{cl}(\omega)$ and $G(\omega)$ we obtained is reasonable and can be used to generate the time-dependent electronic coupling via Eq.(2) and Eq.(5).

With the obtained electronic coupling fluctuation $V_{ij}(t)$, the energy transfer dynamics can be calculated with the similar approach for the diagonal disorder. The obtained rate becomes 3.456×10^{12} s^{-1}, which is smaller than the rate of pure diagonal disorder. This may be explained by the periodical dynamic off-diagonal fluctuation. Compared to the previous analysis [11], in which the rate will be enhanced for the electronic coupling having a linear or Gaussian dependence on the nuclear coordinates, the present result manifests that the rate can be decreased by the fluctuation. Therefore, the fluctuation of the electronic coupling plays a versatile role in the rate calculation.

IV. CONCLUSION

In this work, we mainly investigate the triplet-triplet energy transfer in fluorene dimer by combining the rate theory with electronic structure calculations. Since the electronic coupling and reorganization energy are two key parameters for the control of energy transfer, the accuracy of calculating the two parameters becomes very important. Thus, we test different methods to find out an easy, yet accurate way for calculating the electronic coupling and reorganization energy and the constrained density functional theory is chosen to localize the diabatic triplet states. The rate constant is then calculated by the perturbation theory and wavepacket diffusion approach. It is found that the approaches based on the perturbation limit, such as Marcus formula and Fermi's golden rule, begin to lose their validity for the present system. Especially, the electronic coupling fluctuation decreases the rate compared to the static one for the present system, which is opposite to the fluctuation caused by linear or Gaussian dependence on the nuclear coordinates. Therefore, the fluctuation of the electronic coupling plays a versatile role in the rate calculation.

V. ACKNOWLEDGMENTS

This work was supported by the National Natural Science Foundation of China (No.20833004 and No.21073146) and the Research Fund for the Doctoral Program of Higher Education of China (No.200803840009).

DOI:10.1088/1674-0068/24/05/538-546

[1] W. C. Galley and L. Stryer, Proc. Natl. Acad. Sci. USA **60**, 108 (1968).
[2] M. Wohlgenannt, K. Tandon, S. Mazumdar, S. Ramasesha, and Z. V. Vardeny, Nature **409**, 494 (2001).
[3] H. Zemel and B. M. Hoffman, J. Am. Chem. Soc. **103**, 1192 (1981).
[4] J. L. Bredás, D. Beljonne, V. Coropceanu, and J. Cornil, Chem. Rev. **104**, 4971 (2004).
[5] M. P. Eng and B. Albinsson, Angew. Chem. Int. Ed. **46**, 5626 (2006).
[6] Z. E. X. Dance, M. J. Ahrens, A. M. Vega, A. B. Ricks, D. W. McCamant, M. A. Rater, and M. R. Wasielewski, J. Am. Chem. Soc. **130**, 830 (2008).
[7] A. C. Benniston and A. Harriman, Chem. Soc. Rev. **35**, 169 (2006).
[8] J. V. Weis, S. H. Abdelwahed, R. Shukla, R. Rathore, M. A. Ratner, and M. R. Wasielewski, Science **328**, 1547 (2010).
[9] A. A. Voityuk, J. Phys. Chem. C **114**, 20236 (2010).
[10] T. Alessandro, Chem. Soc. Rev. **40**, 2347 (2011).
[11] Y. Zhao and W. Z. Liang, J. Chem. Phys. **130**, 034111 (2009).
[12] C. P. Hsu, Z. Q. You, and H. C. Chen, J. Phys. Chem. C **112**, 1204 (2008).
[13] Q. Wu and T. V. Voorhis, Phys. Rev. A **72**, 024502 (2005).
[14] T. V. Voorhis, T. Kowalczyk, B. Kaduk, L. P. Wang, C. L. Cheng, and Q. Wu, Annu. Rev. Phys. Chem. **61**, 149 (2010).
[15] H. Haken and P. Reineker, Z. Phys. **249**, 253 (1972).
[16] Y. C. Cheng and R. J. Silbey, Phys. Rev. A **69**, 052325 (2004).
[17] M. Shinozuka, J. Acoust. Soc. Am. **49**, 357 (1971).
[18] M. Shinozuka, Comput. Struct. **2**, 855 (1972).
[19] K. Y. R. Billah and M. Shinozuka, Phys. Rev. A **42**, 7492 (1990).
[20] S. A. Egorov, K. F. Everitt, and J. L. Skinner, J. Phys. Chem. A **103**, 9494 (1999).
[21] H. Tal-Ezer and R. Kosloff, J. Chem. Phys. **81**, 3967 (1984).
[22] C. Leforestier, R. H. Bisseling, C. Cerjan, M. D. Feit, R. Friesner, A. Guldberg, A. Hammerich, G. Jolicard, W. Karrlein, H. D. Meyer, N. Lipkin, O. Roncero, and R. Kosloff, J. Comput. Phys. **94**, 59 (1991).
[23] M. Thoss, H. Wang, and W. H. Miller, J. Chem. Phys. **115**, 2991 (2001).
[24] S. F. Nelsen, S. C. Blackstock and Y. Kim, J. Am. Chem. Soc. **109**, 677 (1987).
[25] W. W. Zhang, W. J. Zhu, W. Z. Liang, Y. Zhao, and S. F. Nelsen, J. Phys. Chem. B **112**, 11079 (2008).
[26] H. M. Qin, X. X. Zhong, Y. B. Si, W. W. Zhang, and Y. Zhao, J. Phys. Chem. A **115**, 3116 (2011).
[27] E. Lee, E. S. Medvedev, and A. A. Stuchebrukhov, J. Chem. Phys. **112**, 9015 (2000).
[28] H. Hwang and P. J. Rossky, J. Phys. Chem. B **108**, 6723 (2004).
[29] A. M. Mebel, Y. T. Chen, and S. H. Lin, Chem. Phys. Lett. **258**, 53 (1996).
[30] W. Z. Liang, Y. Zhao, J. Sun, J. Song, S. L. Hu, and J. L. Yang, J. Phys. Chem. B **110**, 9908 (2006).
[31] M. M. Han, Y. Zhao, and W. Z. Liang, J. Mol. Struct.: THEOCHEM **819**, 13 (2007).
[32] D. A. Case, T. A. Darden, T. E. Cheatham III, C. L. Simmerling, J. Wang, R. E. Duke, R. Luo, R. C. Walker, W. Zhang, K. M. Merz, B. Roberts, B. Wang, S. Hayik, A. Roitberg, G. Seabra, I. Kolossvai, K. F. Wong, F. Paesani, J. Vanicek, J. Liu, X. Wu, S. R. Brozell, T. Steinbrecher, H. Gohlke, Q. Cai, X. Ye, J. Wang, M. J. Hsieh, G. Cui, D. R. Roe, D. H. Mathews, M. G. Seetin, C. Sagui, V. Babin, T. Luchko, S. Gusarov, A. Kovalenko, and P. A. Kollman, *AMBER 11*, San Francisco: University of California, (2010).
[33] M. J. Frisch, G. W. Trucks, H. B. Schlegel, G. E. Scuseria, M. A. Robb, J. R. Cheeseman, G. Scalmani, V. Barone, B. Mennucci, G. A. Petersson, H. Nakatsuji, M. Caricato, X. Li, H. P. Hratchian, A. F. Izmaylov, J. Bloino, G. Zheng, J. L. Sonnenberg, M. Hada, M. Ehara, K. Toyota, R. Fukuda, J. Hasegawa, M. Ishida, T. Nakajima, Y. Honda, O. Kitao, H. Nakai, T. Vreven, J. A. Montgomery Jr., J. E. Peralta, F. Ogliaro, M. Bearpark, J. J. Heyd, E. Brothers, K. N. Kudin, V. N. Staroverov, T. Keith, R. Kobayashi, J. Normand, K. Raghavachari, A. Rendell, J. C. Burant, S. S. Iyengar, J. Tomasi, M. Cossi, N. Rega, J. M. Millam, M. Klene, J. E. Knox, J. B. Cross, V. Bakken, C. Adamo, J. Jaramillo, R. Gomperts, R. E. Stratmann, O. Yazyev, A. J. Austin, R. Cammi, C. Pomelli, J. W. Ochterski, R. L. Martin, K. Morokuma, V. G. Zakrzewski, G. A. Voth, P. Salvador, J. J. Dannenberg, S. Dapprich, A. D. Daniels, O. Farkas, J. B. Foresman, J. V. Ortiz, J. Cioslowski, and D. J. Fox, *Gaussian 09 Program*, Wallingford CT: Gaussian, Inc., (2010).
[34] C. I. Bayly, P. Cieplak, W. D. Cornell, and P. A. Kollman, J. Phys. Chem. **97**, 10269 (1993).
[35] J. Wang, R. M. Wolf, J. W. Caldwell, P. A. Kollman, and D. A. Case, J. Comput. Chem. **25**, 1157 (2004).
[36] Z. Q. You and C. P. Hsu, J. Chem. Phys. **133**, 074105 (2010).
[37] T. Schwabe and S. Grimme, Phys. Chem. Chem. Phys. **9**, 3397 (2007).
[38] S. F. Sousa, P. A. Fernandes, and M. J. Ramos, J. Phys. Chem. A **111**, 10439 (2007).
[39] A. J. Cohen, P. Mori-Sánchez, and W. T. Yang, Science **321**, 792 (2008).
[40] J. D. Chai and M. Head-Gordon, Phys. Chem. Chem. Phys. **10**, 6615 (2008).
[41] Y. Zhao and D. G. Truhlar, Acc. Chem. Res. **41**, 157 (2008).
[42] Y. Shao, L. Fusti-Molnar, Y. Jung, J. Kussmann, C. Ochsenfeld, S. T. Brown, A. T. B. Gilbert, L. V. Slipchenko, S. V. Levchenko, D. P. O'Neill, R. A. DiStasio Jr., R. C. Lochan, T. Wang, G. J. O. Beran, N. A. Besley, J. M. Herbert, C. Y. Lin, T. Van Voorhis, S. H. Chien, A. Sodt, R. P. Steele, V. A. Rassolov, P. E. Maslen, P. P. Korambath, R. D. Adamson, B. Austin, J. Baker, E. F. C. Byrd, H. Dachsel, R. J. Doerksen, A. Dreuw, B. D. Dunietz, A. D. Dutoi, T. R. Furlani, S. R. Gwaltney, A. Heyden, S. Hirata, C. P. Hsu, G. Kedziora, R. Z. Khaliullin, P. Klunzinger, A. M. Lee, M. S. Lee, W. Liang, I. Lotan, N. Nair, B. Peters, E. I. Proynov, P. A. Pieniazek, Y. M. Rhee, J. Ritchie, E. Rosta, C. D. Sherrill, A. C. Simmonett, J. E. Subotnik, H. L. Woodcock III, W. Zhang, A. T. Bell, A. K. Chakraborty, D. M. Chipman, F. J. Keil, A. Warshel,

DOI:10.1088/1674-0068/24/05/538-546

W. J. Hehre, H. F. Schaefer III, J. Kong, A. I. Krylov, P. M. W. Gill, and M. Head-Gordon, Phys. Chem. Chem. Phys. **8**, 3172 (2006).
[43] M. Valiev, E. J. Bylaska, N. Govind, K. Kowalski, T. P. Straatsma, H. J. J. van Dam, D. Wang, J. Nieplocha, E. Apra, T. L. Windus, and W. A. de Jong, Comput. Phys. Commun. **181**, 1477 (2010).
[44] A. D. Becke, J. Chem. Phys. **88**, 2547 (1988).
[45] S. Yeganeh and T. V. Voorhis, J. Phys. Chem. C **114**, 20756 (2010).
[46] Q. Wu and T. V. Voorhis, J. Chem. Theory Comput. **2**, 765 (2006).
[47] F. Gao, W. Z. Liang, and Y. Zhao, J. Phys. Chem. A **113**, 12847 (2009).
[48] F. Pan, F. Gao, W. Z. Liang, and Y. Zhao, J. Phys. Chem. B **113**, 12581 (2009).
[49] R. A. Marcus, J. Phys. Chem. **67**, 853 (1963).
[50] R. A. Marcus and N. Sutin, Biochim. Biophys. Acta **811**, 265 (1985).
[51] S. H. Lin, C. H. Chang, K. K. Liang, R. Chang, Y. J. Shiu, J. M. Zhang, T. S. Yang, M. Hayashi, and F. C. Hsu, Adv. Chem. Phys. **121**, 1 (2002).
[52] Y. Zhao, W. Liang, and H. Nakamura, J. Phys. Chem. A **110**, 8204 (2006).
[53] J. Olofsson and S. Larsson, J. Phys. Chem. B **105**, 10398 (2001).

DOI:10.1088/1674-0068/24/05/538-546